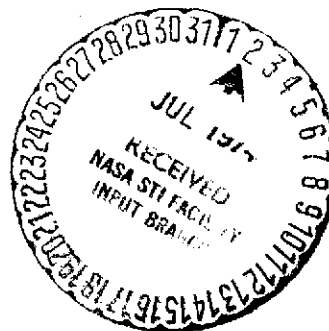




COMPUTER ANALYSIS OF AIRCRAFT AND SHUTTLE ANTENNAS

W. D. Burnside
J. H. Richmond



The Ohio State University
ElectroScience Laboratory

Department of Electrical Engineering
Columbus, Ohio 43212

SEMIANNUAL STATUS REPORT 2902-16
(15 November 1973 to 15 May 1974)

Grant Number NGL 36-008-138

June 1974

(NASA-CX-138605) COMPUTER ANALYSIS OF
AIRCRAFT AND SHUTTLE ANTENNAS Semiannual
Status Report, 15 Nov. 1973 - 15 May
1974 (Ohio State Univ.) 12 p HC \$4.00

N74-26666

Unclas
CSCL 17B G3/07 41302

National Aeronautics and Space Administration
Langley Research Center
Hampton, Va. 23365

COMPUTER ANALYSIS OF AIRCRAFT AND SHUTTLE ANTENNAS

W. D. Burnside
J. H. Richmond

SEMIANNUAL STATUS REPORT 2902-16
(15 November 1973 to 15 May 1974)

Grant Number NGL 36-008-138

June 1974

National Aeronautics and Space Administration
Langley Research Center
Hampton, Va. 23365

/

ABSTRACT

Progress is reported on predicting the patterns of high-frequency antennas on aircraft and shuttles. Patterns are presented for an axial slot antenna on a circular cylinder partially coated with a dielectric layer. Results are presented for Omega signal disturbance by a conducting vertical pole.

TABLE OF CONTENTS

	Page
I. AIRCRAFT AND SHUTTLE ANTENNAS	1
II. DIELECTRIC-FILLED SLOT ANTENNA	3
III. OMEGA SIGNAL DISTURBANCE	7
REFERENCES	8

COMPUTER ANALYSIS OF AIRCRAFT AND SHUTTLE ANTENNAS

I. AIRCRAFT AND SHUTTLE ANTENNAS

During the past six months, the calculated patterns made on the KC-135 aircraft have been completed and compare very favorably with measured results taken at NASA Langley. The results of this study will be presented at the next IEEE Conference[1]. More recently, we have concentrated on collecting shuttle data on a model which is similar to the actual shuttle design. The patterns for various antennas and locations have been measured at NASA Langley on a scale model. The calculated patterns are being generated with some of the results illustrated in Figs. 1 and 2. These results are for antennas located forward of the

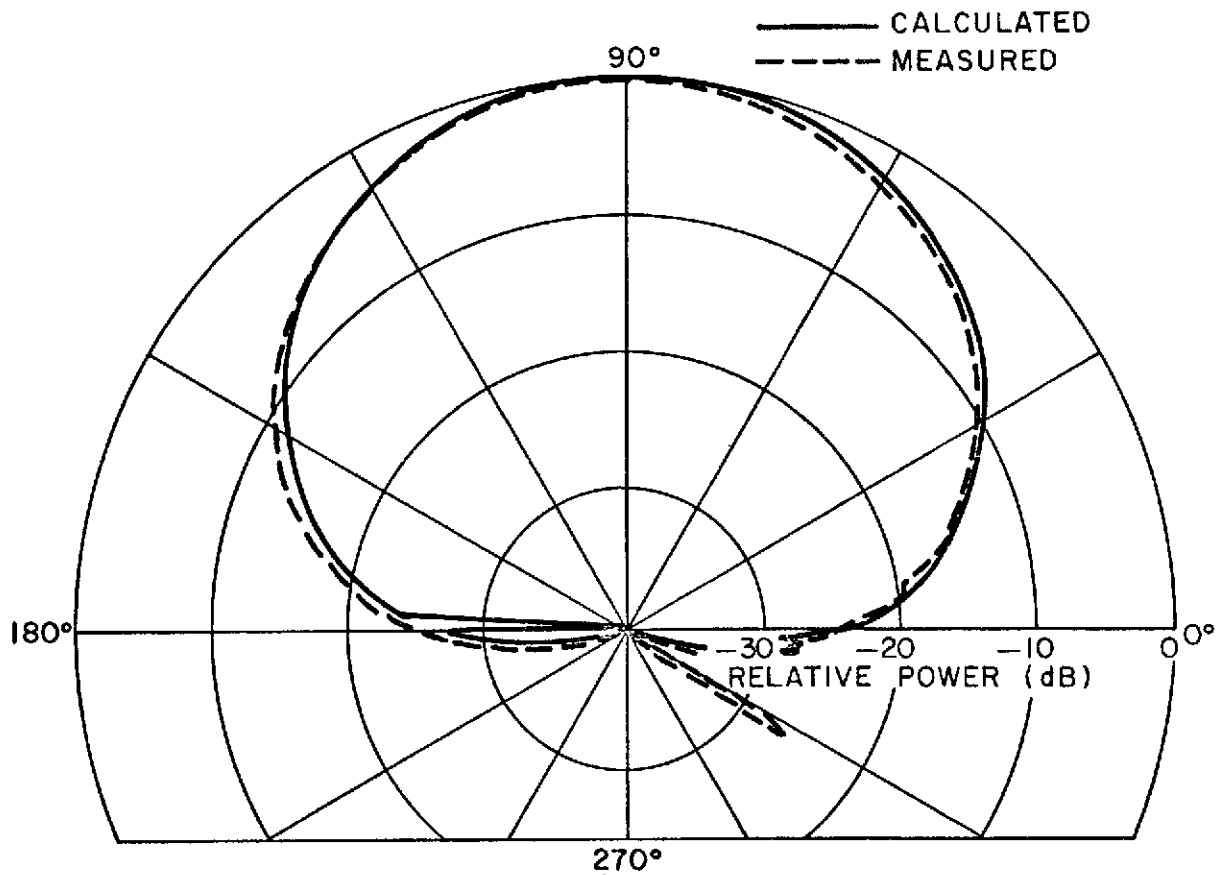


Fig. 1. Roll plane pattern of a circumferential waveguide antenna mounted forward of the wings and atop a scale model shuttle spacecraft.

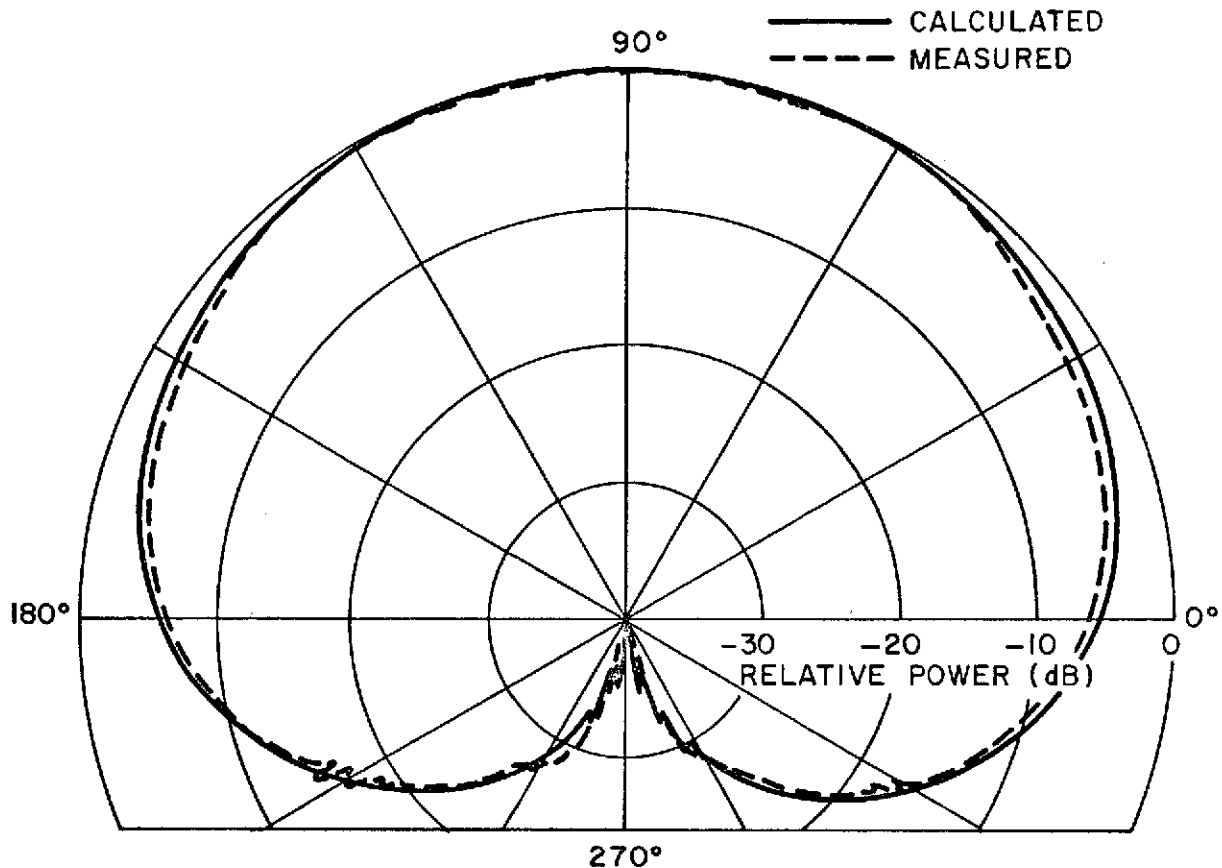


Fig. 2. Roll plane pattern of an axial waveguide antenna mounted forward of the wings and atop a scale model shuttle spacecraft.

wings, whereas the future results will be for antennas mounted over the wings. In addition, patterns have been measured and calculated for antennas mounted on a scale model of the final shuttle design. These results include the effects of the large booster rockets which are mounted below the shuttle, and in each case the agreement between the calculated and measured results is quite good.

The future work in the area of high frequency antenna pattern analysis involves completing the shuttle study for the antennas mounted over the wings. In addition, a study will be initiated on the airborne antennas which might be applied for the microwave landing system. To date, the polarization used for this system has not been finalized and has been a topic of much discussion. It is our goal to aid in this decision by examining the airborne antenna system complexity for each polarization. The antenna systems generated will be those necessary for the desired coverage.

II. DIELECTRIC-FILLED SLOT ANTENNA

In a previous reporting period, we developed a computer program for an axial slot antenna radiating through a flush-mounted dielectric window in a conducting cylinder as in Fig. 3. In the current reporting period,

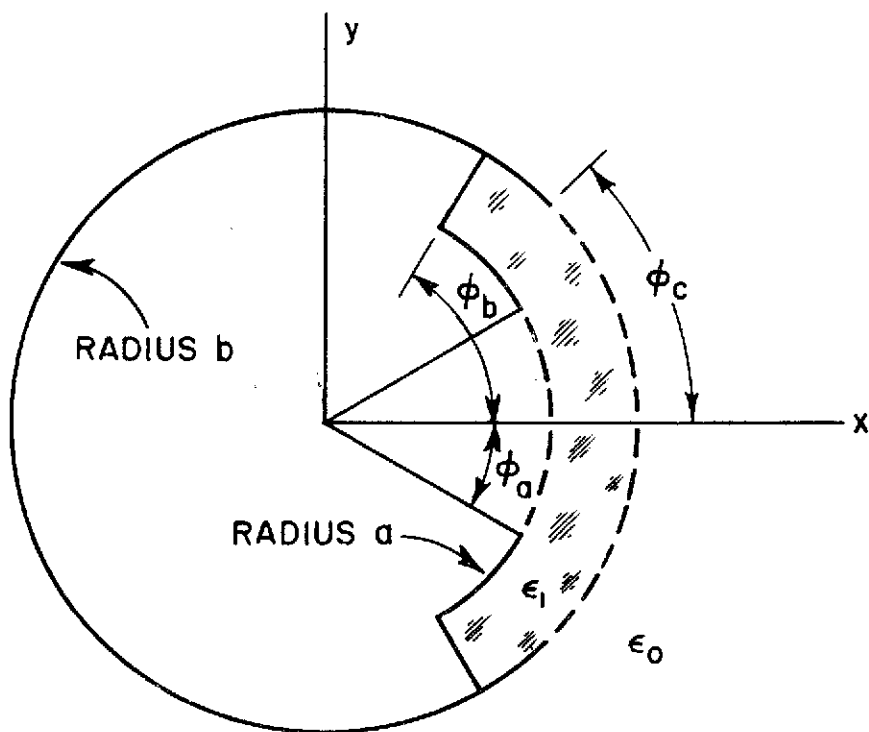


Fig. 3. An axial-slot antenna radiates through a flush-mounted dielectric window in a conducting circular cylinder. The principal field components are E_ϕ and H_z .

the program was improved to handle larger cylinders and higher dielectric constants. Figures 4, 5 and 6 illustrate the far-field patterns with dielectric constants of 2, 3 and 4. The patterns in Figs. 4 and 6 are reasonably smooth, but in Fig. 5 the pattern breaks up into many lobes with deep nulls. With a dielectric constant of 3, this undesirable type of pattern is obtained when the aperture half-angle is $\phi_b = 13.8, 14.8, 15.8, 16.8^\circ$, etc. When ϕ_b differs from one of these critical angles by more than 0.1 degrees, the pattern becomes smooth again. At each critical angle, the aperture width is an integral number of wavelengths for the lowest-order surface wave.

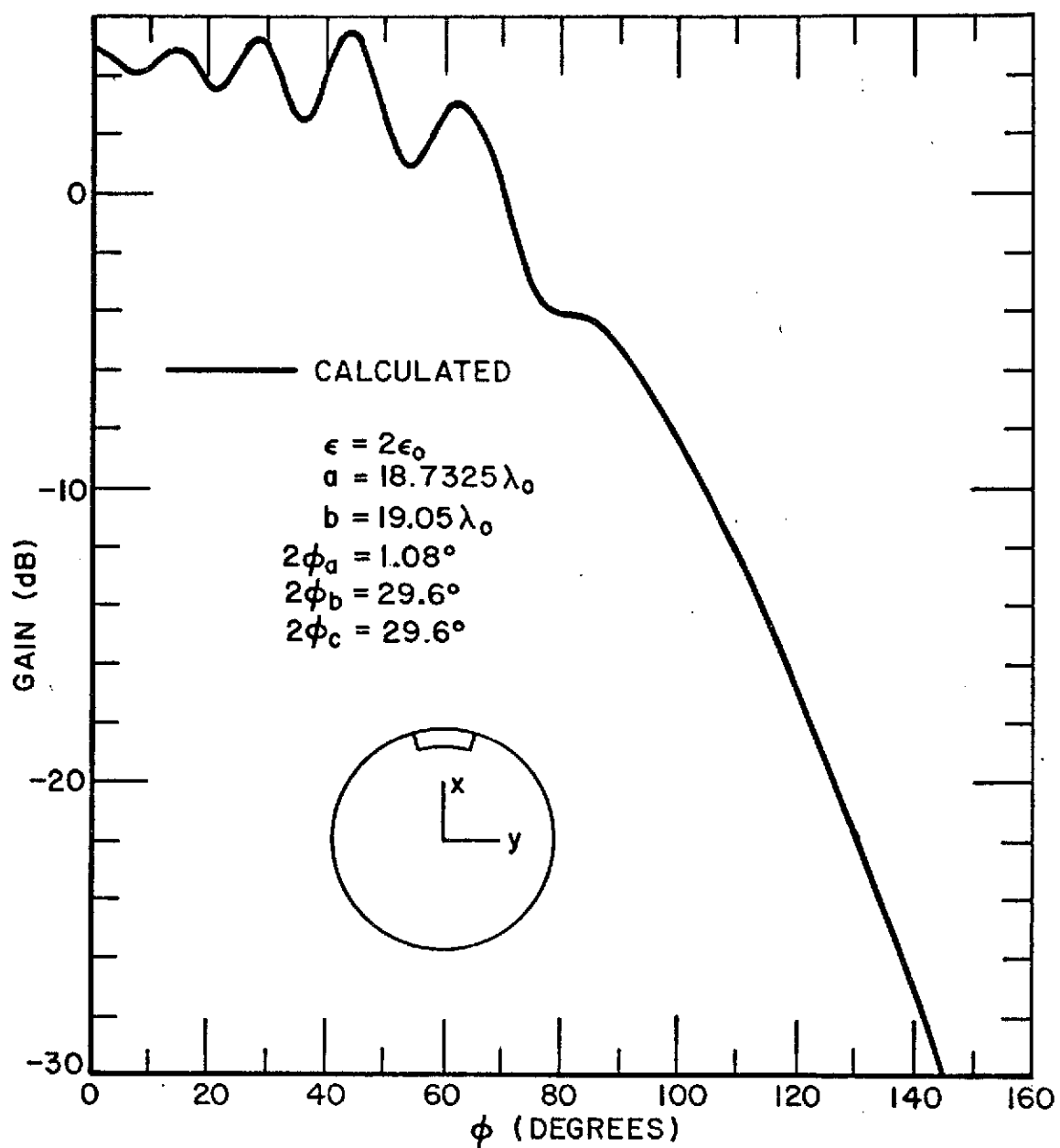


Fig. 4. Far-field pattern of TE axial slot radiating through a flush-mounted dielectric window in a circular cylinder. The dielectric constant is 2.

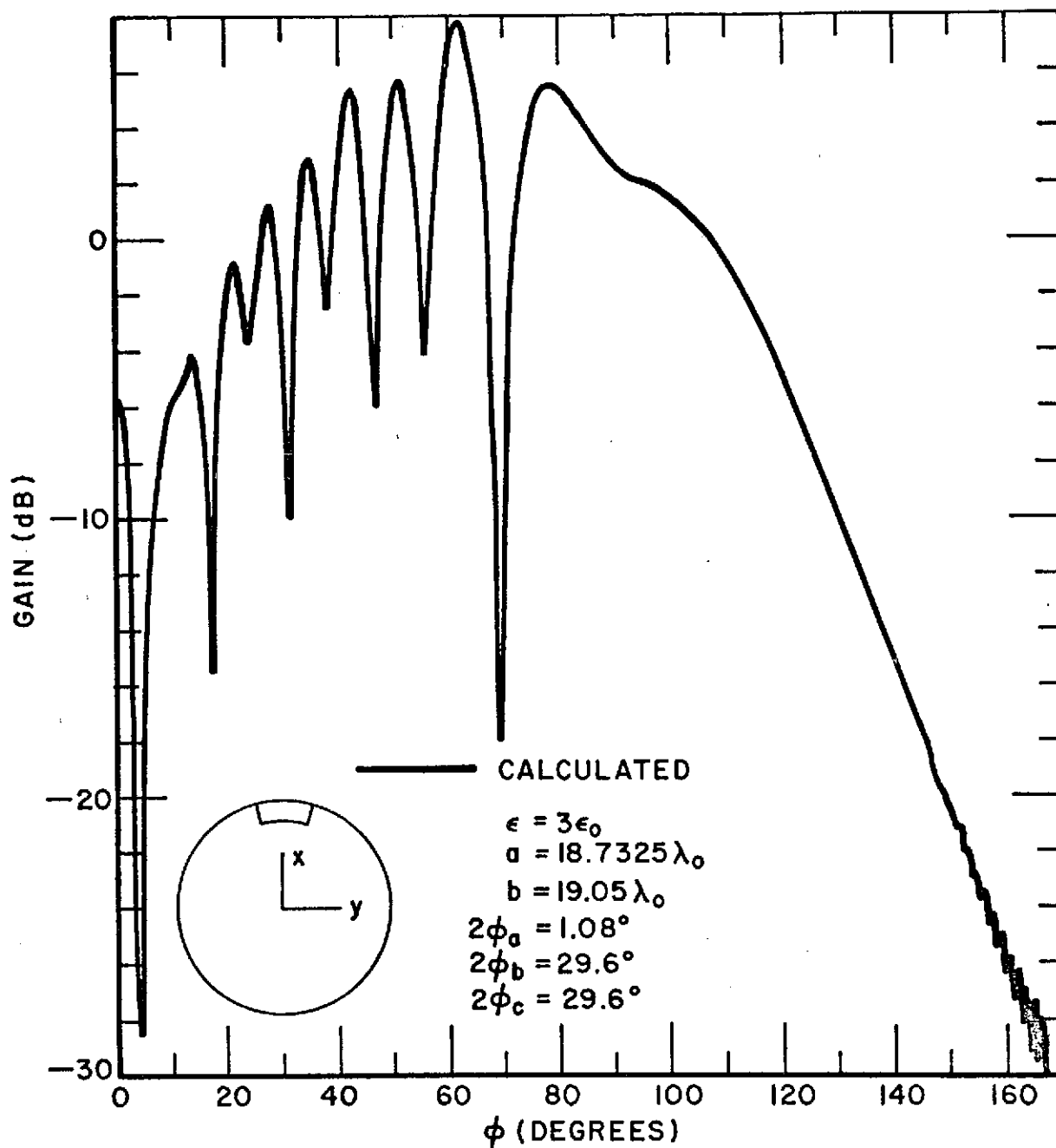


Fig. 5. Far-field pattern of TE axial slot radiating through a flush-mounted dielectric window in a circular cylinder. The dielectric constant is 3.

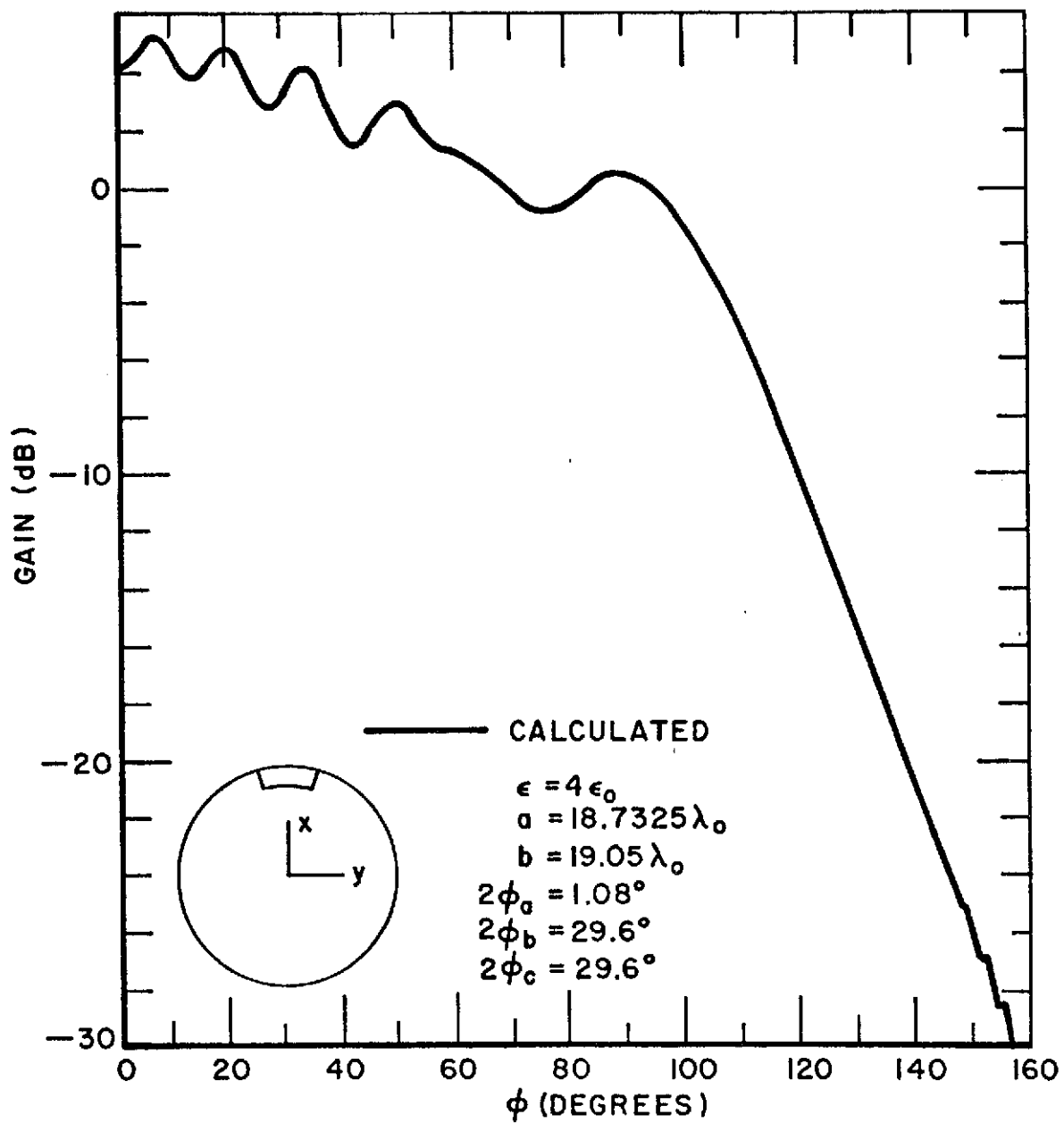


Fig. 6. Far-field pattern of TE axial slot radiating through a flush-mounted dielectric window in a circular cylinder. The dielectric constant is 4.

This surface-wave resonance phenomenon is less pronounced with a dielectric constant of 1.2 but is observed when $\phi_b = 14.6^\circ$. The effect may be reduced with a lossy dielectric window or by reducing the reflections at the edges of the aperture.

In Figs. 4, 5 and 6, the calculations are based on a two-dimensional model with an infinitely long axial slot in an infinitely-long cylinder. A case of greater interest is a half-wave axial slot in a long cylinder. The effects of surface-wave resonance will be smaller for a slot of finite length.

III. OMEGA SIGNAL DISTURBANCE

The Omega navigation system uses vertically polarized waves with a frequency of 10 KHz. Experimental measurements show significant phase variations in the signal in the vicinity of trees, towers and power lines. There is a possibility, however, that these phase disturbances arise from local variations in surface impedance rather than the nearby obstacles.

In our initial investigation of this problem, we considered a vertically polarized plane wave propagating along a horizontal path over a perfectly conducting flat earth. This wave illuminates a perfectly conducting vertical pole with a height of 100 feet. The base of the pole is located at the ground plane and makes contact with it. The radius of the pole is 0.1 feet.

At 10 KHz, the height of the pole is 0.001λ . Using image theory, we may consider the plane wave to have broadside incidence on a 200 foot pole in free space. The current induced on the pole has essentially a cosine distribution with maximum current at the base. If the incident wave has a field strength of one volt per meter, the base current is 0.000267 amperes. The current leads the incident field by 90° . In the extreme near zone the scattered field E_z leads the current by 90° , and E_z is thus 180° out of phase with the incident field. The total field E_z is weak in the vicinity of the pole and vanishes at its surface. The pole does not significantly disturb the phase of the Omega signal in the near zone or the far zone. (A phase shift of much less than one degree is considered insignificant.)

For broadside backscatter, the pole has an echo area of 0.67×10^{-16} square wavelengths. As a center-fed dipole antenna, the 200 foot pole has a terminal impedance $Z = 0.0008 - j 110,000$ ohms.

In this study we found that the standard thin-wire programs are inadequate for scattering by a pole as short as 0.001λ . Therefore, we developed new programs for thin-wire problems in the Rayleigh region. The new programs give consistent results when the pole is divided into 4, 6, 8 or 10 segments. New subroutines were developed for near-zone field analysis, and identical results were obtained with two independent programs.

In the next period we plan to investigate Omega signal disturbances in the vicinity of a tree (modeled as a lossy dielectric pole) and an overhead power transmission cable.

REFERENCES

1. Burnside, W.D., Marhefka, R.J. and Yu, C.L., "A Study of KC-135 Aircraft Antenna Patterns," presented at 1974 International IEEE/APS Symposium at Atlanta, Georgia, June 1974.